DOI: 10.61782/fa.2025.0476

FORUM ACUSTICUM EURONOISE 2025

Initial Analytical Attempts to Handle the Sound Absorption using Segmented Oblique Perforations

Tommaso D'Orazio[1] **Denilson Ramos**[2] **Luís Godinho**[2]
Claudia Guattari[1] **Francesco Asdrubali**[3]
[1] Roma TRE University, Department of Philosophy, Communication and Performing Arts, Via Ostiense 139, 00154 Rome, Italy
[2] Universidade de Coimbra, ISISE, ARISE, Departamento de Engenharia Civil, Rua Luis Reis dos Santos,
3030-788 Coimbra, Portugal
[3] Department of International Human and Social Sciences, Perugia Foreigners' University, Piazza B. Fortebraccio 4, 06123 Perugia, Italy

ABSTRACT

This research presents a novel geometric configuration for acoustic metamaterials designed to optimize sound absorption, particularly at low frequencies. The design introduces a segmented pathway composed of two sections, creating an effective acoustic path longer than the linear distance between the sound wave entry point and the cavity access. This configuration maximizes absorption while maintaining a constant overall thickness.
The study explores various geometric configurations by adjusting the angles of the segmented pathway to enhance absorption at specific frequencies. The research integrates analytical analyses based on the transfer matrix method implemented in MATLAB. A prototype fabricated through 3D printing provides experimental validation of the findings. Preliminary results indicate that tuning the angles of the segmented pathway significantly improves acoustic absorption, offering new possibilities for applications in noise control and architectural acoustics.

*Corresponding author: tommaso.dorazio@uniroma3.it

Keywords: *fluid equivalent model, acoustic metamaterials, sound absorption.*

1. INTRODUCTION

Acoustic metamaterials (AMMs) are designed to optimize sound absorption, particularly at low frequencies. Traditional configurations consist of a flat rigid surface with circular holes or slits, where the neck is typically a single, linear, and straight segment [1]. Sound attenuation primarily occurs due to viscous friction within the pores, while the combination of the neck and the cavity allows for resonance phenomena to enhance absorption. For this reason, resonant absorbers are widely used in architectural acoustics. However, optimizing absorption at low frequencies remains a complex challenge, as the effectiveness of passive absorbers is constrained by the size required to interact with long acoustic wavelengths. Various strategies have been proposed to lower the resonance frequency, such as increasing panel thickness, reducing the diameter of the perforations, or decreasing the overall porosity [2,3]. Although these solutions are effective, they present limitations related to bulkiness, manufacturing costs, and compatibility with compact spaces.
Recent studies have demonstrated that tilting the perforations can shift the resonance frequency to lower values and increase the acoustic absorption coefficient [4,5]. To this end, this research investigates two different

approaches to predict the acoustic properties of materials with segmented pores divided into two inclined sections, contributing to the design of more efficient devices.
This study is structured as follows: Section 2.1 presents the modeling approach and discusses the geometric description of the acoustic metamaterial's unit cell. Section 2.2 describes the analytical method based on the transfer matrix method implemented in MATLAB. Section 2.3 details the experimental procedure, following ISO 10534-2 [6], to characterize the sound absorption properties of the proposed metamaterial. Subsequently, Section 3 presents a comparison of the preliminary results obtained. Finally, Section 4 discusses the main conclusions.

2. GENERAL DESCRIPTION

2.1 Unit Cell Description

The alternative studied in this article introduces a single neck, but divided into two inclined segments, creating a structured geometric configuration. In this design, the first segment forms an entry angle with the external surface, while the second segment, connected to the first, generates a transition angle that alters its direction. Finally, the neck terminates with an exit angle inside the resonant cavity. This configuration extends the effective length of the neck without increasing the overall system thickness, thereby optimizing absorption at low frequencies.
Figure 1 illustrates the geometric dimensions of the resonator in cross-section. Here, r and R_w represent the perforation radius and the impedance tube radius, respectively; L is the resonator thickness; D and R_c denote the cavity depth and radius, respectively; while θ_1 and θ_2 correspond to the inclination of the first segment relative to the incidence surface and the inclination of the second segment relative to the cavity surface. The linear lengths of the first and second segments, L_1 and L_2, are:

$$L_1 = \frac{L}{\frac{\cot(\theta_2)}{\cot(\theta_1)}+1}\frac{\cot(\theta_2)}{\cot(\theta_1)} \quad (1)$$

$$L_2 = \frac{L}{\frac{\cot(\theta_1)}{\cot(\theta_2)}+1}\frac{\cot(\theta_1)}{\cot(\theta_2)} \quad (2)$$

While the effective lengths of the first and second segments, d_1 and d_2, are:

$$d_1 = \frac{L\cos(\theta_2)}{\sin(\theta_1+\theta_2)} \quad (3)$$

$$d_2 = \frac{L\cos(\theta_1)}{\sin(\theta_1+\theta_2)} \quad (4)$$

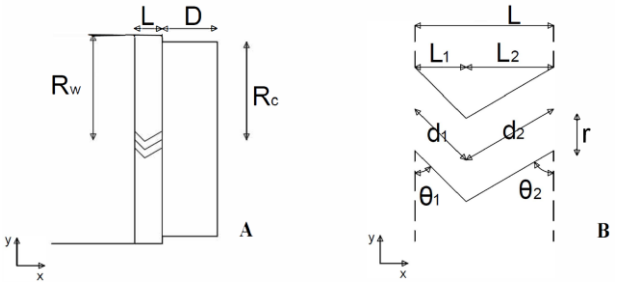

Figure 1. Schematic cross-sectional representation of the proposed resonator with the indication of the main geometric parameters. Figure 1a (left) illustrates the overall configuration of the resonator, highlighting the general geometry, the resonant cavity, and the impedance tube. Figure 1b (right) provides a detailed view of the resonator structure alone, emphasizing the configuration of the neck, which is divided into two inclined segments. Additionally, the total thickness (L), the perforation radius (r), and the angles (θ_1, θ_2) of the two neck segments are indicated.

2.2 Analytical model

The analytical model formulated in this study for characterizing the sound wave propagation in the acoustic metamaterial (AMM) employs the transfer matrix method [7] and the equivalent fluid approach of Johnson-Champoux-Allard (JCA) [8], with the analytical estimation of transport parameters adapted from Atalla and Sgard [3]. To investigate the acoustic properties of the proposed absorber, a theoretical model based on the equivalent fluid theory was developed, treating the perforated resonator as a homogeneous medium with fluid equivalent acoustic properties. This approach enables the characterization of the absorber's acoustic impedance and its behavior in terms of sound absorption.
The absorption coefficient is calculated as:

$$\alpha = 1 - \left|\frac{T(1,1) - Z_0\,T(2,1)/S_w}{T(1,1) + Z_0\,T(2,1)/S_w}\right|^2 \quad (5)$$

where $T=M_1M_2M_c$ is the transfer matrix, $Z_0=c_0\rho_0$ is the characteristic impedance of air, c_0 is the speed of sound propagation, ρ_0 is the air density, and $S_w=\pi R_w^2$ is the cross-section of the impedance tube.
M_1 and M_2 are the matrices describing the acoustic wave propagation through the first and second inclined segment of the resonator neck:

$$M_i = \begin{bmatrix} \cos(k_i L_i) & jZ_i \sin(k_i L_i) \\ \frac{j}{Z_i} \sin(k_i L_i) & \cos(k_i L_i) \end{bmatrix} \quad (6)$$

with $i=1,2$ where the characteristic impedance of the first and second segment of the neck is $z_i = \sqrt{\rho_i B_i}/\pi r^2$. The matrix describing the acoustic wave propagation through the air cavity of the resonator is:

$$M_c = \begin{bmatrix} \cos(k_0 D) & j\frac{Z_0}{S_c} \sin(k_0 D) \\ \frac{jS_c}{Z_0} \sin(k_0 D) & \cos(k_0 D) \end{bmatrix} \quad (7)$$

$S_c = \pi R_c^2$ is the cross-section of the cavity, the wavenumber of air is $k_0 = \omega/c_0$ and the wavenumber of the first and second segment is $k_i = \omega(\rho_i/B_i)^{\frac{1}{2}}$ where ω is the frequency. Initially, in the model herein developed, each region can be homogenized as function of equivalent density ρ_i [8]:

$$\rho_i = \rho_0 \alpha_{\infty i} \left(1 + \frac{\sigma_i \phi_i}{j\omega\rho_0 \alpha_{\infty i}} G_i\right) \quad (8)$$

$$G_i = \sqrt{1 + \frac{4j{\alpha_{\infty i}}^2 \rho_0 \omega}{\lambda^2 {\sigma_i}^2 {\phi_i}^2}} \quad (9)$$

with viscous and thermal characteristic length $\lambda = r/2$. The subscript i describe the effective density in the first and second perforation segments, respectively.

The geometric tortuosity $\alpha_{\infty,i}$ of the first and second neck segments [3]:

$$\alpha_{\infty i} = \frac{1}{\sin^2(\theta_i)} + 2\frac{\varepsilon_{ei}}{d_i} \quad (10)$$

with $\varepsilon_{ei} = 0.85 r F_{ei}$ and $F_{ei} = 1 - 1.4092\xi_i + 0.33818\xi_i^3 + 0.06793\xi_i^5 - 0.02287\xi_i^6 + 0.03015\xi_i^7 - 0.01641\xi_i^8$ with $\xi_i = (\Phi_i)^{1/2}$ is the Fork function [9]. The flow resistance of the first and second neck segments is described as [3]:

$$\sigma_i = \frac{(2d_i/r)sin^2(\theta_i)+4}{d_i \Phi_i} Rs + \frac{8\eta}{\phi_i \left(\frac{r}{2}\right)^2 \cos^2(\theta_i)} \quad (11)$$

where η is the dynamic viscosity of air and $Rs = \frac{\sqrt{2\eta\rho_0\omega}}{2}$. $\Phi_1 = S/S_w$ is the open porosity of the first segment of the neck, where $S = \pi r^2$ and the open porosity of the second segment is $\Phi_2 = 1$, since the radii of the first and second perforation are equal.

The effective compressibility in the first and second segments is [8]:

$$B_i = \frac{\gamma P_0}{\Phi_i} [\gamma - (\gamma - 1)(1 - HG')^{-1}]^{-1} \quad (12)$$

$$H = \frac{8\eta}{j\lambda^2 Pr\omega\rho_n} \quad (13)$$

$$G' = \sqrt{1 + \frac{jPr\omega\rho_0\lambda^2}{16\eta}} \quad (14)$$

where γ is the ratio of specific heats of air, P_0 is the static air pressure, and $Pr = 0.71$ is the Prandtl number for air.

2.3 Experimental Model

To validate the theoretical model introduced in this research, experimental tests were conducted in the laboratory using an impedance tube. The samples were manufactured through an additive manufacturing process at the *Institute for Sustainability and Innovation in Structural Engineering (ISISE)*, within the Department of Civil Engineering at the University of Coimbra. Considering recent advancements in 3D printing techniques for acoustic metamaterials (AMMs) [10], these acoustic metamaterials were designed using advanced computer-aided design (CAD) software and fabricated through a *Fused Deposition Modelling (FDM)* process. The 3D printing process was carried out using a *Blocks One MK2* printer. The *Fused Deposition Modelling (FDM)* method involves melting a thermoplastic filament composed of polylactic acid (PLA), with a diameter of 1.75 mm, at a temperature of 210°C. The molten filament is extruded through a heated 0.4 mm nozzle and systematically deposited layer by layer onto a print platform maintained at 50°C. The 3D-printed samples, shown in Fig. 2, feature a circular configuration with a nominal outer radius R_w of 18.75 mm (Fig. 2a), precisely designed to fit perfectly within a 37,5 mm impedance tube. The actual thicknesses of the specimens, with nominal values (L) of 5 mm and 10 mm, are shown in Fig. 2b and Fig. 2c, respectively.

Figure 2. Sample of the proposed AMM.

Table 1 summarizes the actual thickness (L) dimensions of the six tested samples.

Table 1. Thickness (L) measurements of the printed samples expressed in millimeters.

Sample	L
45°-45°	5,16
60°-45°	5,30
30°-60°	5,28
45°-45°	10,22
60°-45°	10,23
30°-60°	10,28

For this evaluation, the measurement procedure was carried out using the previously described small-scale samples under controlled conditions. The sound absorption and reflection coefficients were measured using the two-microphone technique, employing the transfer function method, in accordance with ISO 10534-2 [6]. The measurement apparatus consists of a closed tube with a sound source that emits a sine-sweep signal generated by a loudspeaker, thereby exciting the system within its operational frequency range. Specifically, for a circular tube with an internal radius of R_w = 18,75 mm, the operational frequency range is between 200 Hz and 4800 Hz. The measurement process of the acoustic pressure measured by microphones p_1 and p_2, positioned at points x_1 and x_2 inside the tube, can be described as follows:

$$P_1 = |p_i|e^{jkx_1} + |p_r|e^{-jkx_1} \quad (15)$$

$$P_2 = |p_i|e^{jkx_2} + |p_r|e^{-jkx_2} \quad (16)$$

where $|p_i|$ and $|p_r|$ represent the amplitudes of the incident and reflected wave pressures on the sample surface, respectively. The transfer functions H_i and H_r, considering each component of the total pressure, can be expressed as follows:

$$H_i = \frac{p_i e^{jkx_2}}{p_i e^{-jkx_1}} = e^{jks} \quad (17)$$

$$H_r = \frac{p_r e^{jkx_2}}{p_r e^{-jkx_1}} = e^{-jks} \quad (18)$$

where $s = x_2 - x_1$. Consequently, the transfer function between the two microphones, H_{12}, is defined as:

$$H_{12} = \frac{p_2}{p_1} = \frac{e^{jkx_2} + Re^{-jkx_2}}{e^{jkx_1} + Re^{-jkx_1}} \quad (19)$$

where R is the complex reflection coefficient, which, as a function of H_{12}, can be expressed as:

$$R = \frac{H_{12} + H_i}{H_r - H_{12}} e^{2jkx_1} \quad (20)$$

The sound absorption coefficient can then be calculated for normal incidence using the following relation: $\alpha = 1 - |R|^2$. This formulation allows for the determination of the sample's acoustic absorption based on the measurement of the transfer function between the two microphones, following the standardized method outlined in ISO 10534-2 [6].

3. PRELIMANARY RESULTS

In the experimental tests, three different unit cell geometries were analyzed, characterized by angles (θ_1 and θ_2) of 45°-45°, 60°-45°, and 30°-60°, respectively. For each configuration, two different variants of nominal thickness (L), 5 mm and 10 mm, and two nominal cavity depth (D) configurations, also 5 mm and 10 mm, were tested. The experimental results obtained in the laboratory were compared and validated using the analytical model. The latter was implemented using the (L) values measured directly from the samples, as reported in Table 1.

Figure 3 shows the comparison between the analytical predictions and the experimental data for the absorption coefficient as a function of frequency. The envelope observed in the analytical graphs is attributed to the uncertainty in the exact measurement of the sample neck radius r. To account for potential inaccuracies due to the printing process, an error margin of 0.05% of the nominal radius of 3 mm was introduced, allowing for possible variations in the actual radius.

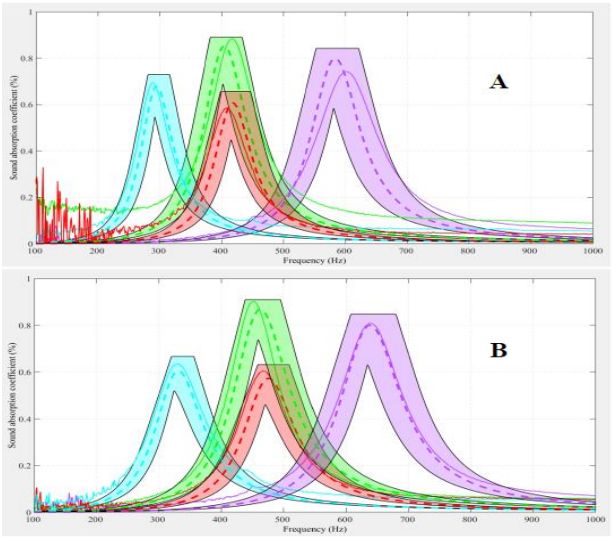

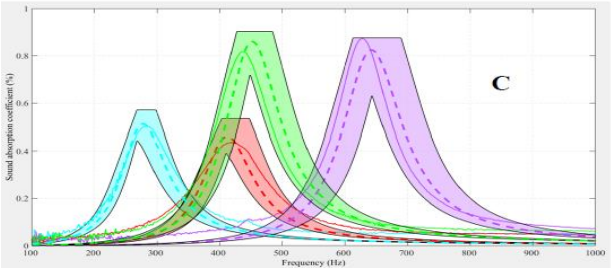

Figure 3. Comparison between experimental and analytical results for the acoustic absorption coefficient as a function of frequency with different geometric configurations of AMMs. Graph (A) corresponds to the configuration with angles 45°-45°, (B) to the 60°-45° configuration, and (C) to the 30°-60° configuration. The colored curves represent different combinations of thickness (L) and cavity depth (D): blue indicates L = 10 mm, D = 10 mm; red L = 10 mm, D = 5 mm; green L = 5 mm, D = 10 mm; and purple L = 5mm, D = 5 mm. Solid lines represent the experimental results, while dashed lines indicate the analytical results obtained for a perforation radius of r = 3 mm. The envelope accounts for a ±5% variation in the perforation radius.

4. CONCLUSIONS

The article explored the study of different unit cell geometries for an acoustic metamaterial resonator (AMM), examining the influence of variations in thickness (L), cavity depth (D), and angles (θ_1 and θ_2) on the geometric configuration of individual cells. The absorption values of the unit cells were validated both through an analytical model using the transfer matrix method [7] and the Johnson-Champoux-Allard (JCA) equivalent fluid approach [8] and through experimental measurements conducted according to the guidelines of ISO 10534-2 [6] on 3D-printed samples. The results demonstrated a significative agreement between the experimental data and analytical predictions, highlighting how variations in geometric characteristics influence both the resonance frequencies and the absorption coefficient amplitudes. This opens space to future investigations about optimised panels handling the segmented necks.

5. ACKNOWLEDGEMENTS

This work was partly financed by FCT / MCTES through national funds (PIDDAC) under the R&D Unit Institute for Sustainability and Innovation in Structural Engineering (ISISE), under reference UID/04029/Institute for Sustainability and Innovation in Structural Engineering (ISISE), and under the Associate Laboratory Advanced Production and Intelligent Systems ARISE under reference LA/P/0112/2020.

6. REFERENCES

[1] P. Ruggeri, F. Peron, N. Granzotto, and P. Bonfiglio, “Analisi sperimentale parametrica sull’assorbimento acustico di risonatori acustici a cavità,” in *Proc. of the 41st National Conference of the Italian Acoustical Association (AIA)*, Pisa, Italy, 2014.

[2] D. Y. Maa: “Noise control using perforated panel absorbers,” *Noise Control Eng. J.*, vol. 29, no. 3, pp. 77–84, 1987.

[3] N. Atalla and F. Sgard: “Acoustic modeling of porous materials,” *J. Sound Vib.*, vol. 303, pp. 195–208, 2007

[4] J. Carbajo, S. Ghaffari Mosanenzadeh, S. Kim, and N. X. Fang, “Sound absorption of acoustic resonators with oblique perforations,” *Appl. Phys. Lett.*, vol. 116, no. 5, pp. 054101, 2020.

[5] K. Attenborough: “Sound absorption in porous materials with inclined pores,” *Appl. Acoust.*, vol. 130, pp. 188–194, 2018.

[6] International Organization for Standardization: *ISO 10534-2:1998 Acoustics — Determination of sound absorption coefficient and impedance in impedance tubes — Part 2: Transfer-function method*. Geneva, Switzerland: ISO, 1998.

[7] M. Munjal: *Acoustics of Ducts and Mufflers*. New York: Wiley, 2014. ISBN: 978-1-118-44309-5.

[8] J. Allard and N. Atalla: *Propagation of Sound in Porous Media: Modelling Sound Absorbing Materials*. New York: Wiley, 2009. ISBN: 978-0-470-74734-6.

[9] Jaouen, L., Chevillotte, F. “Length correction of 2D discontinuities or perforations at large wavelengths and for linear acoustics”, *Acta Acustica United with Acustica*, vol. 104, pp. 243-250, 2018.

[10] T. G. Zieliński, N. Dauchez, T. Boutin, et al.: "Taking advantage of a 3D printing imperfection in the development of sound-absorbing materials," *Applied Acoustics*, vol. 197, pp. 108941, 2022. ISSN: 0003-682X. doi: 10.1016/j.apacoust.2022.108941.